

Fractional Derivatives Embody Essential Features of Cell Rheological Behavior

VLADAN D. DJORDJEVIĆ,¹ JOVO JARIĆ,² BEN FABRY,³ JEFFREY J. FREDBERG,³
and DIMITRIJE STAMENOVIC⁴

¹Faculty of Mechanical Engineering, ²Faculty of Mathematics, University of Belgrade, Serbia and Montenegro, ³Physiology Program, Harvard School of Public Health, Boston, MA, and ⁴Department of Biomedical Engineering, Boston University Boston, MA

(Received 4 November 2002; accepted 23 February 2003)

Abstract—Mechanical moduli of cultured airway smooth muscle cells (Fabry, B., *et al. Phys. Rev. Lett.* 87:148102, 2001) reveal that the frequency dependence of cell rheological behavior conforms to a weak power-law relationship over a wide range of frequency (10^{-2} – 10^3 Hz). Such a behavior cannot be accounted for by standard viscoelastic models characterized by a discrete number of time constants that have been commonly used in previous studies of cell viscoelasticity. Fractional calculus, by contrast, provides a natural framework for describing weak power-law relationships and requires no assumptions about the type of material, the time constant distribution or the time/frequency interval in which rheological observations are made. In this study, we developed a rheological model of the cell using methods of fractional calculus. We used a least-squares technique to fit the model to data previously obtained from measurements on airway smooth muscle cells. The fit provided an excellent correspondence to the data, and the estimated values of model parameters were physically plausible. The model leads to a novel and unexpected empirical link between dynamic viscoelastic behavior of the cytoskeleton and the static contractile stress that it bears. © 2003 Biomedical Engineering Society. [DOI: 10.1114/1.1574026]

Keywords—Power law, Elastic modulus, Frictional modulus, Frequency, Modeling, Contractile force.

INTRODUCTION

Rheological measurements on living cells have shown that cell behavior is viscoelastic. Earlier techniques (e.g., micropipette aspiration, magnetic cytometry, micromanipulation) measured the ongoing deformations in response to a step change in stress, or the creep response,^{3,14,21} and the ongoing changes in stress in response to a step change in deformation, or the stress relaxation.¹⁸ These measurements were usually interpreted in terms of simple viscoelastic models characterized by a discrete number of time constants. Recent developments of oscillatory magnetic cytometry call into

question the appropriateness of using these types of models for describing the cell rheological behavior, however. Measurements of mechanical moduli over a wide range of forcing frequencies (10^{-2} – 10^3 Hz) in cultured airway smooth muscle cells have revealed the following features.⁶ The elastic (storage) modulus (G') increases with increasing frequency according to a weak power law with a power-law exponent of about 0.2. The frictional (loss) modulus (G'') also follows the power law for at least three decades (10^{-2} – 10^1 Hz), but at higher frequencies this dependence increases and approaches a power-law exponent of 1 at very high frequencies, which, in turn, indicates Newtonian fluid behavior. This power-law dependence implies that the cell rheological behavior is not determined by specific molecular mechanisms, but rather might reflect a generic property of the integrated system.

Fabry and colleagues⁶ have shown that the observed power-law behavior of cells conforms closely to the following empirically based relationships:

$$(a) \quad G' = G_0 \left(\frac{\omega}{\Phi_0} \right)^k \Gamma(1-k) \cos \frac{\pi k}{2}$$

and

$$(b) \quad G'' = G_0 \left(\frac{\omega}{\Phi_0} \right)^k \Gamma(1-k) \sin \frac{\pi k}{2} + \omega \mu, \quad (1)$$

where ω is the circular (radian) frequency, G_0 and Φ_0 are scaling factors for stiffness and frequency, respectively, k is the power-law exponent ($0 \leq k < 1$), μ is a coefficient of Newtonian viscous damping and $\Gamma(\cdot)$ is the gamma function. When $k=0$, $G'=G_0$, and $G''=\omega\mu$, and hence, when $\omega \rightarrow 0$ the cell rheological behavior approaches that of Hookean elastic materials. In the limit $k \rightarrow 1^-$, $G' \rightarrow 0$, and $G'' \sim \omega$, i.e., the behavior

Address correspondence to Dimitrije Stamenović, Department of Biomedical Engineering, Boston University, 44 Cummington Street, Boston, MA 02215. Electronic mail: dimitrij@engc.bu.edu

of Newtonian fluids. Thus, the earlier relationships describe the transition from a solid-like ($k=0$) to a fluid-like ($k=1$) rheological behavior of cells. The authors provided an intriguing physical interpretation of the observed behavior of the cells based on the theory of soft glassy materials (see Discussion).

It has been shown that a rheological behavior that conforms to the power law can be described by using methods of fractional calculus.^{1,11,13,16,19} In this study we used principles of fractional calculus to develop a mathematical model of cell rheological behavior. To illustrate the applicability of this model, we analyzed the data for oscillatory behavior of cultured airway smooth muscle cells obtained previously.⁶ We discuss our results in the light of the theory of soft glassy materials and the notion that the cell is organized as a stress-supported structure.

BASICS OF FRACTIONAL CALCULUS AND ITS APPLICATION TO RHEOLOGY

Riemann's definition of the fractional derivative of a function $f(\cdot)$ is given as follows:¹²

$$D_t^{(\alpha)}(f) \equiv \frac{1}{\Gamma(1-\alpha)} \frac{d}{dt} \int_0^t \frac{f(\tau)}{(t-\tau)^\alpha} d\tau, \quad (2)$$

where t is an independent variable, $0 \leq \alpha < 1$ represents the order of the derivative, and $\Gamma(\cdot)$ is the gamma function. A key difference between the classical (integer-order) derivative and the fractional derivative is that the former represents a local property of a function, whereas the latter represents a global property of a function within a given closed interval $[0, t]$.

During the past decades fractional calculus has found a wide application in various branches of science and engineering including transport phenomena, probability, and economics. However, fractional calculus has enjoyed greatest success in the field of rheology. The reason for this is that fundamental properties of the fractional derivative appear to be a natural framework for describing the material behavior that conforms to a power law.

Suppose that pure shear behavior of a material is described as follows:

$$T \propto D_t^{(\alpha)}(\gamma), \quad (3)$$

where T is shear stress, $\gamma(t)$ is the corresponding shear strain, and t is time. Since, by definition, the fractional derivative represents a global property, then the right-hand side of Eq. (3) is indicative of a change in γ throughout history of deformation. This is different from the case of an integer-order derivative that would indicate only the current change in γ . When $\alpha=0$, it follows from Eqs. (2) and (3) that $T \propto D_t^{(0)}(\gamma) = \dot{\gamma}(t)$, providing

$\dot{\gamma}(0)=0$; the proportionality between the stress and strain implies the elastic Hookean behavior. When $\alpha=1$, the fractional derivative is not defined. However, it can be shown, using the Laplace transform, that in the limit when $\alpha \rightarrow 1^-$, $T \propto D_t^{(\alpha)}(\gamma) \rightarrow \dot{\gamma}(t)$ where the dot denotes the first time derivative; the proportionality between the stress and the rate of strain ($\dot{\gamma}$) implies the Newtonian viscous behavior. Thus, when $0 < \alpha < 1$, Eq. (3) describes a rheological behavior which is neither purely elastic nor viscous. In this respect the order of the fractional derivative α is analogous to the power exponent k from Eqs. (1a) and (1b). By transforming Eq. (3) into the frequency domain using the Fourier transform one can obtain a relationship that conforms to a weak power-law behavior with α being the power-law exponent (see the next section).

MODELING

A general rheological model based on fractional derivatives is described as follows:¹¹

$$T + bD_t^{(\beta)}(T) = G_s \gamma + \sum_{i=1}^n \lambda_i D_t^{(\alpha_i)}(\gamma), \quad (4)$$

where the variables have the same meaning as in Eq. (3), b and λ_i s are constants, G_s is a static elastic modulus, $0 \leq \beta < 1$ and $0 \leq \alpha_1 < \alpha_2 < \dots < \alpha_n < 1$ are orders of the fractional derivatives. In the case of $n=1$, $b=0$, and $\alpha_1=1$, Eq. (4) becomes the equation of motion for the Kelvin–Voigt linear viscoelastic model. In the case of $n=1$ and $\alpha_1=\beta=1$, Eq. (4) becomes the equation for the standard linear solid. If, in addition, $\lambda_1=0$, Eq. (4) reduces to the Maxwell model. The most frequently used rheological model with fractional derivatives is so-called generalized Zener model^{1,11,19} which can be obtained from Eq. (4) by setting $n=1$. It has been shown¹ that for reasons of thermodynamic consistency (i.e., the second law of thermodynamics) the following constraints have to be imposed on the model parameters: $\alpha_1=\beta$, $G_s \geq 0$, $\lambda_1 > 0$, $b > 0$, and $\lambda_1/b > G_s$ so that the model contains only four independent parameters. Recently, a model that has two fractional derivatives ($n=2$) on the right-hand side of Eq. (4) such that $\alpha_1=\beta$ was proposed.¹³ It was shown that in this model the thermodynamic constraints on the model parameters are more relaxed than in the previous model, i.e., $\alpha_2 > \beta$ and $\lambda_1/b > G_s$; the later condition holds even when $b=0$.

Model of cell rheology. In this study we describe previously published data⁶ for the rheological behavior of cultured airway smooth muscle cells during forced oscillations from 10^{-2} – 10^3 Hz using a fractional derivative model. These data exhibit a weak power-law behavior; in the case of G' this behavior extends over the

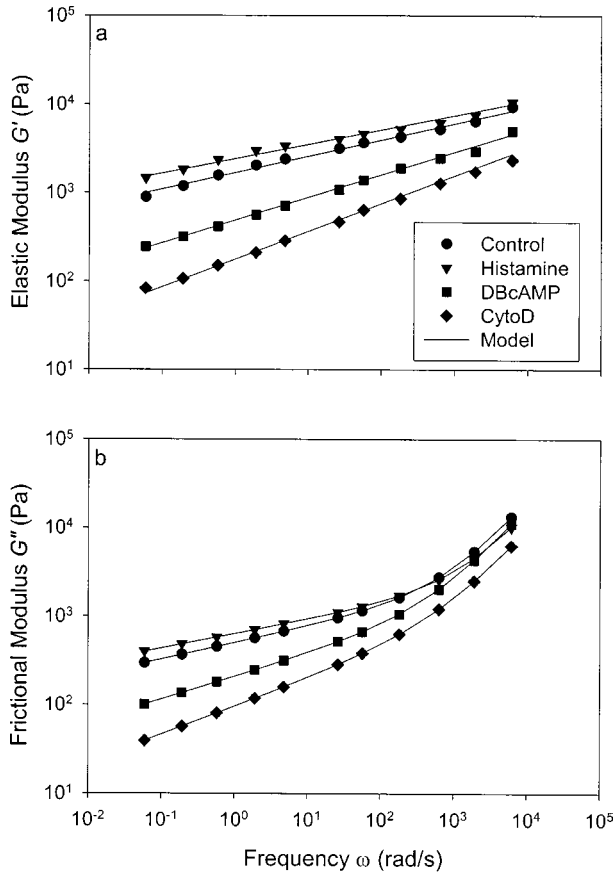


FIGURE 1. (a) Elastic (storage) modulus (G') and (b) frictional (loss) modulus (G'') measured in cultured airway smooth muscle cells increase with increasing circular frequency (ω) following a weak power law. Above ~ 100 rad/s, the dependence G'' vs. ω increases and asymptotically approaches the slope of unity at high frequencies. Different symbols correspond to different cell stimulations: controls, constrictor histamine (10^{-4} M), relaxant (DBcAMP, 10^{-3} M) and actin disruptor cytoschalasin D (CytoD, 2×10^{-6} M). Adopted from data of Fabry *et al.* (see Ref. 6). The theoretical Eqs. (12a) and (12b) provide a good correspondence to these data.

observed frequency range whereas in the case of G'' the power-law behavior is observable below 10 Hz but at higher frequencies G'' asymptotically approaches the behavior that characterizes Newtonian fluids (Fig. 1). To our knowledge this behavior of G'' at high frequencies has not been considered previously in fractional derivative models. In this study we incorporated this behavior in the model of the cell.

We started from the general model given by Eq. (4). We transformed this equation from the time domain into the frequency domain using the Fourier integral transform, $F[\cdot]$. Taking into account that the Fourier transform of the fractional derivative of a function f is $F[D_t^{(\alpha)}(f)] = (i\omega)^\alpha F[f]$, we obtained that $F[T] = G^* F[\gamma]$, where $G^* = G' + iG''$ is the complex (dy-

namic) modulus and $i = \sqrt{-1}$ is the imaginary unit. It was found that

$$G^* = \frac{G_s + \sum_{i=1}^n \lambda_i (i\omega)^{\alpha_i}}{1 + b(i\omega)^\beta}. \quad (5)$$

Taking the imaginary part of Eq. (5), we obtained that in the limit of $\omega \rightarrow \infty$:

$$G'' \sim \frac{\lambda_n}{b} \omega^{\alpha_n - \beta} \sin(\alpha_n - \beta) \frac{\pi}{2} \quad (6)$$

when $b \neq 0$, and

$$G'' \sim \lambda_n \omega^{\alpha_n} \sin \alpha_n \frac{\pi}{2} \quad (7)$$

when $b = 0$. If $b \neq 0$ and $(\alpha_n - \beta) \rightarrow 1$, G'' would assume the observed linear (i.e., Newtonian) dependence on ω [see Eq. (6)]. Since both α_n and β take values between 0 and 1, this condition can be satisfied only when $\beta \rightarrow 0$ and $\alpha_n \rightarrow 1$. In this case the left hand side of Eq. (4) reduces to $(1+b)T$. If, however, we divide Eq. (4) with $(1+b)$, we would obtain an expression which has the same form as if $b = 0$. Based on the earlier considerations we concluded that we could use Eq. (4) to describe the behavior of G'' of the cells at high frequencies only if $b = 0$ and $\alpha_n = 1$.

To simulate the data for the oscillatory behavior of airway smooth muscle cells (Fig. 1), we proposed the simplest model that satisfies the above conditions, i.e., $n = 2$, $b = 0$, $\alpha_2 = 1$, and defined the parameters $\lambda_1 \equiv \lambda$, $\lambda_2 \equiv \mu$, $\alpha_1 \equiv \alpha$ where $0 \leq \alpha < 1$. In this case, Eq. (4) becomes as follows:

$$T = G_s \gamma + \lambda D_t^{(\alpha)}(\gamma) + \mu \dot{\gamma}. \quad (8)$$

By transforming Eq. (8) into the frequency domain using the Fourier integral transform, we obtained the following expressions for G' and G'' :

$$(a) \quad G' = G_s + \lambda \omega^\alpha \cos \frac{\pi \alpha}{2}$$

and

$$(b) \quad G'' = \lambda \omega^\alpha \sin \frac{\pi \alpha}{2} + \omega \mu. \quad (9)$$

According to Eqs. (9a) and (9b), both G' and G'' exhibit a weak power-law dependence on ω . As ω increases, the second term on the right-hand side of Eq. (9b) (i.e., $\omega \mu$)

becomes dominant which, in turn, implies Newtonian viscous behavior characterized by viscous damping μ . In the limit of $\omega=0$, $G'=G_s$, which represents the static elastic modulus.

To completely define the viscoelastic behavior, a model has to be able to describe both stress relaxation and creep time responses in a self-consistent manner. For the input step-strain $\gamma(t)=\gamma_0 H(t)$, where γ_0 is a constant and $H(t)$ is the unit step function, we obtained from Eq. (8) the relaxation modulus, $G(t)=T(t)/\gamma_0$, as follows:

$$G(t)=G_s H(t)+\frac{\lambda}{\Gamma(1-\alpha)}\frac{1}{t^\alpha}+\mu\delta(t), \quad (10)$$

where $\delta(t)$ is the delta function. It follows from Eq. (10) that for $t>0$ $G(t)$ decays according to a weak power-law $t^{-\alpha}$ and asymptotically approaches the static elastic modulus G_s as $t\rightarrow\infty$. For $t=0$, $G(0)\rightarrow\infty$ (i.e., rigid body behavior).

The creep response was obtained by assuming the input step-stress, $T=T_0 H(t)$, where T_0 is a constant. This response, however, could not be obtained directly from Eq. (8), but by transforming this equation using the Laplace integral transform and then calculating the creep strain. Taking into account that the Laplace transform, $L[\cdot]$ of a fractional derivative of a function $f(t)$ is $L[D_t^{(\alpha)}]=s^\alpha L[f]$, where s the parameter of the transformation, we obtained from Eq. (8) that

$$L[\gamma]=\frac{T_0}{(G_s+\lambda s^\alpha+\mu s)s}. \quad (11)$$

It is well known that the behavior of the Laplace transform of a function in the limits of $s\rightarrow\infty$ and $s\rightarrow 0$ determines the behavior of the function in the limits of $t\rightarrow 0$ and $t\rightarrow\infty$, respectively: $\lim_{s\rightarrow\infty,0}sL[\gamma]=\lim_{t\rightarrow 0,\infty}\gamma(t)$, providing that these limits exist.⁵ Taking this into account, it follows from Eq. (11) that in the limits of $t\rightarrow 0$ and $t\rightarrow\infty$, the creep compliance, $J\equiv\gamma(t)/T_0$, approaches 0 and $1/G_s$, respectively. [The existence of the limits $\lim_{t\rightarrow 0,\infty}\gamma(t)$ is shown in the Appendix]. Since the theory of linear viscoelasticity demands that in the limits of $t\rightarrow 0$ and $t\rightarrow\infty$ $G(t)=1/J(t)$, it follows from the earlier results that the model can predict the limits of the short and long time response of stress relaxation and creep in a self-consistent manner. For $t=0$, the model predicts a rigid body behavior (i.e., $G\rightarrow\infty$ and $J\rightarrow 0$). Since such behavior is not physically feasible, it follows that the model predictions in the time domain have physical meaning only for $t>0$.

MODEL IMPLEMENTATION AND RESULTS

We used the model, Eq. (8), to describe the oscillatory data of cultured airway smooth muscle cells obtained previously by Fabry *et al.*⁶ Briefly, the measurements were done using the magnetic oscillatory cytometry technique. In these measurements, small (4.5 μm diameter) ferrimagnetic beads were coated with RGD peptide that binds specifically to integrin receptors. The beads (2–3 beads per cell apical surface) were first magnetized by horizontal magnetic field and then twisted by a sinusoidal varying (10^{-2} – 10^3 Hz) vertical magnetic field. From the applied specific torque and measured corresponding bead displacement, the complex (dynamic) stiffness (dimensions stress per unit displacement) was obtained as the ratio of the 2. These data were then transformed into traditional complex (dynamic) modulus G^* (dimensions stress) by multiplying the complex stiffness by a geometric factor that depends on the shape and thickness of the cell and on the degree of bead internalization in the cell.¹⁰ The real part of G^* is G' and the imaginary part is G'' . Measurements were done in control cells, in stimulated cells (10^{-4} M histamine), in relaxed cells [10^{-3} M N⁶,2'-O-dibutyryl adenosine 3',5'-cyclic monophosphate (DBcAMP)], and in cells in which the actin network was disrupted (2×10^{-6} M citochalasin D). (For further details see Fabry *et al.*)⁶

We fitted the model [Eqs. (9a) and (9b)] to the data by minimizing the squared magnitude of the residuals of $\log G^*$ summed over all frequencies and all drug treatments conditions, with the constraint that $G_s\geq 0$. The minimization was performed using Microsoft Excel solver. We obtained a set of values for G_s , λ , α , and μ for each cell treatment condition. We found that the parameter G_s was close to zero for all treatment conditions. Using a reduction-in-variance F-test we found that we could eliminate the parameter G_s altogether without significantly changing the goodness of fit. We introduced additional simplifications into Eqs. (9a) and (9b) by setting $G_s=0$ and $\lambda=\Lambda_0/\Omega_0^\alpha$:

$$(a) \quad G'=\Lambda_0\left(\frac{\omega}{\Omega_0}\right)^\alpha\cos\frac{\pi\alpha}{2}$$

and

$$(b) \quad G''=\Lambda_0\left(\frac{\omega}{\Omega_0}\right)^\alpha\sin\frac{\pi\alpha}{2}+\omega\mu. \quad (12)$$

This allowed us to further reduce the number of parameters by constraining the fit to single values of Λ_0 and Ω_0 that were independent of drug treatment (Fig. 1). We obtained a unique set of values for Λ_0 and Ω_0 whereas the values for α and μ depended upon cell treatment

TABLE 1. Estimated model parameters. Parameter values Λ_0 , Ω_0 , α , and μ obtained by fitting Eqs. (12a) and (12b) to the experimental data of Fabry *et al.* (see Ref. 6). Confidence intervals are given with each parameter value. The values of Λ_0 and Ω_0 are the same for all cell treatments.

Treatment	Λ_0 (kPa)	Ω_0 (rad/s)	α	μ (Pa·s)
Control	38.9 ^{47.2} _{30.7}	2.01 ^{4.87} _{0.83} × 10 ⁷	0.185 ^{0.190} _{0.180}	1.76 ^{1.93} _{1.59}
Histamine			0.164 ^{0.169} _{0.158}	1.23 ^{1.37} _{1.09}
DBcAMP			0.256 ^{0.260} _{0.251}	1.50 ^{1.63} _{1.36}
CytoD			0.313 ^{0.320} _{0.307}	0.78 ^{0.86} _{0.70}

(Table 1). Such obtained values for α and μ were similar to those obtained with Eqs. (9a) and (9b). In both cases, Eqs. (9a) and (9b) and Eqs. (12a) and (12b), estimated values of μ obtained for different drug treatments did not seem to change systematically with drug treatments. However, when the same value of μ was used for all drug treatments, the residual variance increased slightly but significantly ($p < 0.05$).

We analyzed the sensitivity of the fit of Eqs. (12a) and (12b) to variability in the data by determining the 95% confidence interval of the parameter estimates. We observed that the variability in the primary data (G' and G'') between beads at a given frequency and treatment was approximately proportional to the magnitude of G' or G'' , respectively. The underlying log-normal probability function of G' and G'' in airway smooth muscle cells has been analyzed in detail elsewhere.⁶ The logarithmic standard deviation of both G' and G'' measurements was approximately 2.1, regardless of frequency and treatment condition. We then used a Monte Carlo simulation to draw a large number (1000) of random G' and G'' data sets that had the same noise structure as our measurements. We then fitted Eqs. (12a) and (12b) to each data set, and determined the 95% confidence interval of the estimated parameters. The 95% confidence intervals were found to be very narrow, except for estimates of Ω_0 and Λ_0 (Table 1). This is mainly because Ω_0 was far outside (2.01×10^7 rad/s) the frequency range of measurements.

The exponent α exhibited a systematic dependence on cell treatment (Table 1). In stimulated cells α decreased whereas in relaxed cells α increased relative to the base line. In cells with disrupted actin network α decreased even further. This, in turn, suggests that rheological behavior of stimulated cells is closer to the behavior of an elastic solid than that of relaxed cells or cells with disrupted actin network. Such a behavior is consistent with previous observations that cell stiffness is higher in stimulated cells than in relaxed cells.²² This issue and potential mechanisms are further addressed in the Discussion. Newtonian viscous damping coefficient μ did not exhibit a systematic dependence on the cell treatment (Table 1), suggesting that the state of cell contractility

has no direct effect on μ . This is not surprising since if μ were indicative of cell cytoplasmic viscosity, then it should not depend on the extent of contractile stress of the cytoskeleton.

DISCUSSION

In this study we developed a mathematical model based on the principles of fractional calculus to describe the rheological behavior airway smooth muscle cells. The most favorable aspect of this approach is that it represents a natural mathematical framework for describing the power-law behavior that is exhibited by the cells. Such a behavior can be also accounted for by generalized viscoelastic models that are described by hereditary integrals [generalized Maxwell and generalized Kelvin–Voigt models (cf. Fung)].⁷ However, in all such models a distribution of time constants needs to be prescribed empirically, whereas in models with fractional derivatives such a distribution is a consequence of the definition of the fractional derivative. Another advantage of the fractional derivative formulation is that it is described by linear integrodifferential equations. This, in turn, makes possible easy transfer between the time and frequency domains using the Fourier and Laplace integral transforms.

Selection of model parameters was not entirely *ad hoc*. Besides satisfying thermodynamic constrains, values of model parameters were also dictated by the ability of the model to describe the predominantly Newtonian behavior of G'' at high frequencies. The latter feature is a novel result in fractional derivative modeling.

The model predicts a power-law behavior in both frequency, Eqs. (9a) and (9b), and time, Eqs. (10), (A6), and (A12), domains. The model also predicts that as the frequency increases the frictional modulus G'' approaches the behavior of Newtonian fluids, Eq. (9b). The predicted behavior in the frequency domain is consistent with experimentally obtained values from living airway smooth muscle cells. Since this consistency extends over five decades of frequency, we concluded that the model could capture the essential feature of cell rheological behavior. Unpublished studies of the creep behavior of cultured airway smooth muscle cells indicate a power-law time dependence, with a power-law exponent of the creep compliance that closely matched the power-law exponent determined in the frequency domain (G. Lenormand, personal communication). Taken together, these observations are consistent with the model predictions that the power law-dependences during oscillatory loading [Eqs. (9a) and (9b)] and creep [Eqs. (A6) and (A12)] are determined by the same power-law exponent.

Mechanistic Considerations

Fabry and colleagues⁶ offered an intriguing physical interpretation of their data obtained from oscillatory measurements on airway smooth muscle cells. The authors recognized that the observed power-law behavior of cells is consistent with the physics of soft glassy materials.¹⁵ According to this theory, soft glassy materials are composed of discrete elements (whatever they may be) that interact with neighboring elements through the agency of forces that are weak and complex. Each such element is imagined to be trapped in an energy well formed by these neighboring elements, and Φ_0 is taken as an index of the rate at which each element attempts to hop out of its trap. In the presence of sufficient microscale agitation, elements can hop out of one energy well and fall into another. Hopping events such as these lead to a system that is far away from thermodynamic equilibrium with structure that is characterized by disorder and metastability. At the glass transition (i.e., the state when these materials behave as perfect elastic solids) these elements cannot escape their energy wells that are large compared with their local agitation energies. In this case, the effective noise temperature, x , equals unity and the corresponding stiffness is G_0 . When $x > 1$ the elements can escape from their energy wells, however, because local agitation is sufficient to promote hopping between wells. As x increases from $x=1$ to $x=2$, the material undergoes transition from the solid state to the fluid state. Thus, the effective noise x describes transition from the solid to the liquid state analogous to the power-law exponent k from Eqs. (1a) and (1b) and to the order of the fractional derivative α from Eqs. (12a) and (12b), i.e., k and α equal $x-1$. This analogy between k and x led Fabry *et al.*⁶ to the conclusion that the observed oscillatory cell behavior conforms to the theory of soft glassy materials.

To investigate whether our model is consistent with this theory, we set $\Lambda_0 = G_0$, $\Omega_0 = \Phi_0$ and $\alpha = x-1$ into Eqs. (12a) and (12b) and obtained that

$$(a) \quad G' = G_0 \left(\frac{\omega}{\Phi_0} \right)^{x-1} \cos \frac{\pi(x-1)}{2}$$

and

$$(b) \quad G'' = G_0 \left(\frac{\omega}{\Phi_0} \right)^{x-1} \sin \frac{\pi(x-1)}{2} + \omega\mu. \quad (13)$$

When $x=1$, it follows from Eq. (13a) that $G' = G_0$ and that the first term in Eq. (13b) vanishes, i.e., the elastic solid behavior. When $x=2$, it follows from Eq. (13a) that $G' = 0$ and from Eq. (13b) that $G'' \propto \omega$, i.e., the Newtonian fluid behavior. Thus, our model is consistent with the

main facets of the soft glassy rheology. It has been shown recently that adherent cells belong to the class of stress-supported structures.²² Such structures secure static mechanical stability by maintaining a high degree of tension within filamentous structural elements. A hallmark of such structures is that their stiffness is directly attributable to the pre-existing static stress carried by these filamentous elements before load application.²⁰ In the cell, the pre-existing stress is primarily generated by molecular contractile motors, especially myosin II, and is carried by actin filaments. It was found in cultured airway smooth muscle cells that G' is proportional to the maximal cell contractile force (F_{\max})²²:

$$G' = cF_{\max}, \quad (14)$$

where c is a frequency-dependent factor of proportionality. In order for Eqs. (13a) and (14) to be mathematically consistent, than at a given ω their right-hand sides have to be equal. Since for the values of $\alpha = x-1$ obtained by fitting the experimental data (Table 1) $\cos \pi(x-1)/2 \approx 1$, this consistency requirement implies that: $cF_{\max} \approx G_0(\omega/\Phi_0)^{x-1}$. Thus, we obtain the following relationship:

$$x-1 \approx \frac{\log F_{\max} - \log(G_0/c)}{\log(\omega/\Phi_0)}. \quad (15)$$

Since for experimental range of frequencies $\omega \ll \Phi_0$, Eq. (15) implies that $x-1$ must decrease with the logarithm of F_{\max} . Experimental data testing this prediction show close correspondence. Using the values for $\Phi_0 = 2.01 \times 10^7$ rad/s, $G_0 = 38.94$ kPa, and the value for $c = 20.8$ Pa/nN from the literature,²² we predicted from Eq. (15) values for $x-1$ that correspond to F_{\max} of 63.93 and 117.30 nN and to $\omega = 0.628$ rad/s. The values of F_{\max} were measured in cultured airway smooth muscle cells at base line and after stimulation with a saturated dose of histamine (10^{-5} M).²² The predicted values of $x-1$ of 0.195 at baseline and 0.160 after histamine closely correspond to experimentally determined values of α of 0.185 and 0.164, respectively (Table 1). These data lead to a novel and unexpected empirical link between dynamic viscoelastic behavior of the cytoskeleton and the static contractile stress that it bears. They also indicate an intriguing role of the cytoskeletal contractile stress: while it maintains cell's structural stability under applied mechanical loads, it also regulates cell's transition from a solid-like to a fluid-like behavior that is essential for cell's function.

Conclusions

This study showed that fractional calculus is a useful mathematical tool for analyzing rheological properties of cells. It is a natural framework for describing the power-law behavior that has been observed during mechanical measurements on cultured airway smooth muscle cells. Although at this point we have no explanation for the biophysical nature of the fractional derivative, the proposed model leads to a novel relationship which identifies the cytoskeletal contractile stress as a potential regulator of the transition of the cell from a solid-like to a fluid-like behavior. Furthermore, since the power-law behavior is a hallmark of many biological phenomena observed at different scales and at various levels of organization,^{2,4,6,8,9,16,17} fractional calculus offers a unifying mathematical approach to various problems in bioengineering and in biophysics.

ACKNOWLEDGMENTS

The authors thank Dr. Teodor Atanacković and Dr. James P. Butler for helpful discussions. This work was done while Dr. Stamenović was at his sabbatical leave at the Faculty of Mathematics of the University of Belgrade, Serbia and Montenegro. This study was supported by the NIH Grant No. HL-33009. Dr. Djordjević and Dr. Jarić were supported by the Serbian Ministry of Research, Technology and Development through corresponding scientific program Nos. 1373 and 1793.

APPENDIX

The derivations in this Appendix are based on the approach described by Doetsch.⁵

To describe the behavior of strain $\gamma(t)$ in the vicinity of $t=0$, we did the following procedure. In order to expand the Laplace transform of $\gamma(t)$ in a series that converges for large values of s , we rewrote Eq. (11) as follows:

$$L[\gamma] = \frac{T_0}{(G_s + \lambda s^\alpha + \mu s)s} = \frac{T_0}{\mu s^2} \frac{1}{1 + \frac{G_s + \lambda s^\alpha}{\mu s}} \quad (\text{A1})$$

and then expanded the right-hand side of Eq. (A1) as a binomial series

$$L[\gamma] = \frac{T_0}{\mu s^2} \sum_{k=0}^{\infty} (-1)^k \left(\frac{G_s + \lambda s^\alpha}{\mu s} \right)^k. \quad (\text{A2})$$

Using the binomial formula we expanded each member on the right-hand side of Eq. (A2) as follows:

$$\left(\frac{G_s + \lambda s^\alpha}{\mu s} \right)^k = \left(\frac{\lambda}{\mu} \right)^k \frac{1}{s^{(1-\alpha)k}} \sum_{j=0}^k \binom{k}{j} \left(\frac{G_s}{\lambda s^\alpha} \right)^j. \quad (\text{A3})$$

By substituting Eq. (A3) into Eq. (A2), we obtained a series representation of $L[\gamma]$ as follows:

$$L[\gamma] = \frac{T_0}{\mu} \sum_{k=0}^{\infty} \left(-\frac{\lambda}{\mu} \right)^k \sum_{j=0}^k \binom{k}{j} \left(\frac{G_s}{\lambda} \right)^j \frac{1}{s^{2+k-\alpha(k-j)}}. \quad (\text{A4})$$

By taking the inverse Laplace transform of each term on the right-hand side of Eq. (A4) we obtained the strain as a function of time as follows:

$$\gamma(t) = \frac{T_0}{\mu} \sum_{k=0}^{\infty} \left(-\frac{\lambda}{\mu} \right)^k \sum_{j=0}^k \binom{k}{j} \left(\frac{G_s}{\lambda} \right)^j \frac{t^{1+k-\alpha(k-j)}}{\Gamma[2+k-\alpha(k-j)]}. \quad (\text{A5})$$

The first two terms of the series given by Eq. (A5) are

$$\gamma(t) \sim \frac{T_0}{\mu} t \left[1 - \frac{\lambda t^{1-\alpha}}{\mu \Gamma(3-\alpha)} \right] + \text{HOT}, \quad (\text{A6})$$

where HOT indicates higher order terms. Those are multiples of positive powers of t . Thus, it follows from Eq. (A6) that in the limit of $t \rightarrow 0^+$, $\gamma(t) \rightarrow 0$.

To describe the behavior of $\gamma(t)$ for large values of t , we did the following procedure. In order to expand the Laplace transform of $\gamma(t)$ in a series that converges for small values of s , we rewrote Eq. (11) as follows:

$$L[\gamma] = \frac{T_0}{(G_s + \lambda s^\alpha + \mu s)s} = \frac{T_0}{G_s s} \frac{1}{1 + \frac{\lambda}{G_s} s^\alpha + \frac{\mu}{G_s} s}. \quad (\text{A7})$$

We then expanded the right-hand side of Eq. (A7) as a binomial series as follows:

$$L[\gamma] = \frac{T_0}{G_s s} \sum_{k=0}^{\infty} (-1)^k \left(\frac{\lambda}{G_s} s^\alpha + \frac{\mu}{G_s} s \right)^k. \quad (\text{A8})$$

Using the binomial formula, the terms on the right-hand side of Eq. (A8) can be written as follows:

$$\left(\frac{\lambda}{G_s} s^\alpha + \frac{\mu}{G_s} s \right)^k = \left(\frac{\lambda}{G_s} s^\alpha \right)^k \sum_{j=0}^k \binom{k}{j} \left(\frac{\mu}{\lambda} s^{1-\alpha} \right)^j. \quad (\text{A9})$$

By combining Eqs. (A8) and (A9), we obtained the following series representation of $L[\gamma]$:

$$L[\gamma] = \frac{T_0}{G_s} \sum_{k=0}^{\infty} \left(-\frac{\lambda}{G_s} \right)^k \sum_{j=0}^k \binom{k}{j} \left(\frac{\mu}{\lambda} \right)^j \frac{1}{s^{1-\alpha(k-j)-j}}. \quad (\text{A10})$$

By taking the inverse Laplace transform of Eq. (A10), term-by-term, we obtained $\gamma(t)$:

$$\begin{aligned} \gamma(t) = & \frac{T_0}{G_s} \sum_{k=0}^{\infty} \left(-\frac{\lambda}{G_s} \right)^k \sum_{j=0}^k \binom{k}{j} \\ & \times \left(\frac{\mu}{\lambda} \right)^j \frac{1}{\Gamma[1-\alpha(k-j)-j] t^{\alpha(k-j)+j}}. \end{aligned} \quad (\text{A11})$$

The first two terms of the series given by Eq. (A11) are

$$\gamma(t) \sim \frac{T_0}{G_s} \left[1 - \frac{\lambda t^{-\alpha}}{G_s \Gamma(1-\alpha)} \right] + \text{HOT}, \quad (\text{A12})$$

where HOT are negative powers of t . Thus it follows from Eq. (A12) that in the limit of $t \rightarrow \infty$, $\gamma(t) \rightarrow T_0/G_s$.

REFERENCES

- ¹Bagley, R. L. and P. J. Torvik. On the fractional calculus model of viscoelastic behavior. *J. Rheol.* 30:133–155, 1986.
- ²Bates, J. H. T., G. N. Maksym, D. Navajas, and B. Suki. Lung tissue rheology and 1/f noise. *Ann. Biomed. Eng.* 22:674–681, 1994.
- ³Bausch, A. R., F. Ziemann, A. A. Boulbitch, K. Jacobson, and E. Sackmann. Local measurements of viscoelastic parameters of adherent cell surfaces by magnetic bead microrheometry. *Biophys. J.* 75:1573–1583, 1998.
- ⁴Coughlin, M. F., B. Suki, and D. Stamenović. Dynamic behavior of lung parenchyma in shear. *J. Appl. Physiol.* 80:1880–1890, 1996.
- ⁵Doetsch, G. Anleitung zum praktischen Gebrauch der Laplace-Transformation. München, West Germany: R. Oldenbourg, 1961.
- ⁶Fabry, B., G. N. Maksym, J. P. Butler, M. Glogauer, D. Navajas, and J. J. Fredberg. Scaling the microrheology of living cells. *Phys. Rev. Lett.* 87:148102, 2001.
- ⁷Fung, Y. C. Biomechanics: Mechanical Properties of Living Tissues, 2nd ed. New York: Springer, 1993.
- ⁸Hantos, Z., B. Daróczy, B. Suki, S. Nagy, and J. J. Fredberg. Input impedance and peripheral inhomogeneity of dog lungs. *J. Appl. Physiol.* 71:168–178, 1992.
- ⁹Hildebrandt, J. Comparison of mathematical models for cat lung and viscoelastic balloon derived by Laplace transform methods from pressure-volume data. *Bull. Math. Biophys.* 31:651–667, 1969.
- ¹⁰Mijailovich, S. M., M. Kojic, M. Zivkovic, B. Fabry, and J. J. Fredberg. A finite element model of cell deformation during magnetic bead twisting. *J. Appl. Physiol.* 93:1429–1436, 2002.
- ¹¹Pritz, T. Analysis of four-parameter fractional derivative model of real solid materials. *J. Sound Vib.* 195:103–115, 1996.
- ¹²Ross, B. A brief history and exposition of the fundamental theory of fractional calculus. In: *Fractional Calculus and Its Applications*, Lecture Notes in Mathematics 457, edited by A. Dold and B. Eckmann. Berlin: Springer, 1974, pp. 1–36.
- ¹³Rossikhin, Y. A. and M. V. Shitikova. Analysis of dynamic behaviour of viscoelastic rods whose rheological models contain fractional derivatives of two different orders. *Z. Angew. Math. Mech.* 81:363–376, 2001.
- ¹⁴Sato, M., D. P. Theret, L. T. Wheeler, N. Ohshima, and R. M. Nerem. Application of the micropipette technique to the measurements of cultured porcine aortic endothelial cell viscoelastic properties. *ASME J. Biomech. Eng.* 112:263–268, 1990.
- ¹⁵Sollich, P. Rheological constitutive equation for a model of soft glassy materials. *Phys. Rev. E* 58:738–759, 1998.
- ¹⁶Suki, B., A.-L. Barabási, and K. R. Lutchén. Lung tissue viscoelasticity: A mathematical framework and its molecular basis. *J. Appl. Physiol.* 76:168–178, 1994.
- ¹⁷Suki, B., A.-L. Barabási, Z. Hantos, F. Peták, and H. E. Stanley. Avalanches and power-law behavior in lung inflation. *Nature (London)* 368:615–618, 1994.
- ¹⁸Thoumine, O. and A. Ott. Time scale dependent viscoelastic and contractile regimes in fibroblasts probed by microplate manipulation. *J. Cell. Sci.* 110:2109–2116, 1997.
- ¹⁹Torvik, P. J. and R. L. Bagley. On the appearance of the fractional derivative in the behavior of real materials. *ASME J. Appl. Mech.* 51:294–298, 1984.
- ²⁰Volokh, K. Y. and O. Vilnay. New cases of reticulated under-constrained structures. *Int. J. Solids Struct.* 34:1093–1104, 1997.
- ²¹Wang, N. and D. E. Ingber. Control of the cytoskeletal mechanics by extracellular matrix, cell tension, and mechanical stress. *Biophys. J.* 66:2181–2189, 1994.
- ²²Wang, N., I. M. Tolić-Nørrelykke, J. Chen, S. M. Mijailovich, J. P. Butler, J. J. Fredberg, and D. Stamenović. Cell prestress. I. Stiffness and prestress are closely associated in contractile adherent cells. *Am. J. Physiol.* 282:C606–C616, 2002.